SIMULATIONS OF CRYOGENIC SYSTEMS FOR THE SLOW POSITRON PRODUCTION AT ELI – NP

Ion DOBRIN[1], Nikolay DJOURELOV[2], Dan ENACHE[3,4], Alexandru MOREGA[5], Andrei DOBRIN[6], Iuliu POPOVICI[7]

Positron beams are used intensively for materials science and for fundamental topics in applied physics. Within the ELI-NP project, an intense source of moderated positrons will be realized. It is based on the (γ, e^+e^-) reaction, by an intense γ beam interacting with a converter made of high Z-material. The created energetic positrons will be moderated, and the extracted slow positrons will be used to study the surface and near surface zones of a sample. The solid Neon at cryogenic temperatures is the most efficient moderator, known up to now, and it is successfully applied for positron sources based on ^{22}Na system, however, it has been never tested if the neon moderation can work with a γ to e^+ converter system. In the present study, we describe thermal analysis of the two positron source systems. Numerical studies of the thermal loads for the cryocooling system and of the thermal profile of the positron source elements, based on the Finite Element Method, are provided.

Keywords: positron, solid neon moderator, cryogenic simulation, finite element method

1. Introduction

Predicted in 1930 by Dirac [1] and few years later (1933) discovered by Anderson [2], the positron (e^+) has the same mass and spin as the electron, but a positive charge. When interacting with matter, the positrons thermalize (lose

[1]PhD., Senior Researcher I, Head of ASCIE Lab., National Institute for Research and Development in Electrical Engineering ICPE – CA, Bucharest, Romania, e-mail: ion.dobrin@icpe-ca.ro

[2] PhD, Senior Researcher II, Extreme Light Infrastructure — Nuclear Physics, Horia Hulubei National Institute for Physics and Nuclear Engineering, 30 Reactorului Str., 077125 Magurele, Ilfov county, Romania, e-mail: nikolay.djourelov@eli-np.ro

[3] Eng., Ass. Researcher, ASCIE Lab., National Institute for Research and Development in Electrical Engineering ICPE – CA, Bucharest, Romania, Doctoral School of Electrical Engineering at UPB, e-mail: dan.enache@icpe-ca.ro

[4] Ph.D. Student, Dept. of Machines, materials and electrical drive, University POLITEHNICA of Bucharest, Romania

[5] Prof., Dept. of Electrical Machines, Materials and Drives, University POLITEHNICA of Bucharest, Romania, e-mail: alexandru.morega@upb.ro

[6] Eng., Ass. Researcher, ASCIE Lab., National Institute for Research and Development in Electrical Engineering ICPE – CA, Bucharest, Romania, e-mail: andrei.dobrin@icpe-ca.ro

[7] Eng., IDT I, MNE Dept., National Institute for Research and Development in Electrical Engineering ICPE – CA, Bucharest, Romania, e-mail: iuliu.popovici@icpe-ca.ro

energy) in 1 ps time, eventually annihilate electrons, within few ns, are mostly two annihilation rays (E ~ 511 keV) are emitted as a result of the annihilation.

Slow positron beams are created by re-emission of moderated positrons from suitable solids (moderators) bombarded with fast positrons from a positron-emitting radioactive source (*e.g.*, ^{22}Na, ^{58}Co), or created by pair production by bremsstrahlung in a target at electron linear accelerators [3-5] or γ-radiation from nuclear reactors [6-8]. The slow positron beams are successfully used in materials science for studies with positron spectroscopy methods, due to positron high sensitivity in detecting surface and subsurface physical and chemical properties. They become more and more popular as the time of a measurement reduces with the newly available high intensity beams, and also due to the continuous development of moderators with improved efficiency. The moderation efficiency of a moderator material, defined as the number of slow positrons produced per primary fast positron, depends on the positron diffusion length compared to the mean implantation depth of the fast positrons, as well as on the branching ratio for positron emission through the surface [9]. Materials with high energy positron band states favor positron emission and materials with longer positron diffusion length are considered as more efficient moderators. The most efficient moderation (moderator efficiency up to ~ 1%) is obtained with solid rare gas (neon) layer [10].

At ELI-NP, as a part of the systems for gamma beam applications, a positron laboratory will be built. The brilliant low energy gamma beam of very low divergence, which will provide 2.4×10^{10} photons s^{-1} with energies up to 3.5 MeV, will interact with a converter. Earlier studies based on simulations showed that, in case of tungsten converter and if the converter acts as moderator too, the intensity of the slow positron beam can reach 1×10^{6} positrons·s^{-1} [11]. The heat load to the converter/moderator assembly (CMA), as a result of the interaction with the gamma rays, is estimated to be less than 2 mW, which implies that moderation by solid neon is applicable [12]. The CMA is an assembly of thin tungsten foils, mounted on the cold finger of a cryocooler, and it is kept at 5…10 K, suitable for solidification of the neon in ultra-high vacuum (UHV) condition. A successful implementation of the solid neon moderation is expected to increase the slow positron beam intensity to about 2×10^{7} positrons·s^{-1} since the ratio of the neon to tungsten moderation efficiency is ~20. Here, we describe the thermal analysis of the CMA positron source system and that of a standard positron source system using a commercial ^{22}Na emitter of positrons. The latter system, although with at least one order lower intensity, allows year-round operation of the positron laboratory since the devoted time for positron production access to the gamma beam necessary to operate the former system is limited.

Numerical studies based on the Finite Element Method (FEM) of the thermal loads for the cryocooling system and of the thermal profile of the positron source elements are provided and, on this basis, decisions on the choice of

cryocooler types and power are taken.

2. Design of the ^{22}Na Source Chambers

2.1. The conceptual model for the ^{22}Na source chamber

Cryogenic systems for e^+ moderation with solid neon are operational in several laboratories with some variations in the technical implementation either with a closed cycle cryocooler or liquid helium supply [13-16]. The common features are that a copper extension with a conical-like outlet hole is kept at low temperature to freeze neon as thin surface layer. A fraction of the fast e^+ from the source is thermalized in the solid neon layer. Therefore, the thermalized e+ can easily reach the neon-vacuum interface. There, because of the negative e+ work function of solid neon, the thermalized e+ can be injected into the vacuum with an energy of few eV. Weak electric field facilitates the formation of the moderated e^+ beam and an energy filter is used to block the fast e^+. The guidance of the slow e^+ to different spectrometer stations can be magnetic, electrostatic or hybrid. The system is equipped with a neon gas supply system with manual or automatic control in order to obtain an optimum thickness of the solid neon layer. During the introduction of the neon gas, the chamber volume is insulated with gate valves. Once the optimum thickness of the solid neon layer is achieved, the neon gas supply is stopped and the gate valve opens the access to the vacuum pump to sustain the vacuum conditions. The optimum solid neon layer control is indirect by monitoring the count rate of annihilation gamma rays of slow e^+ reaching at a gate valve.

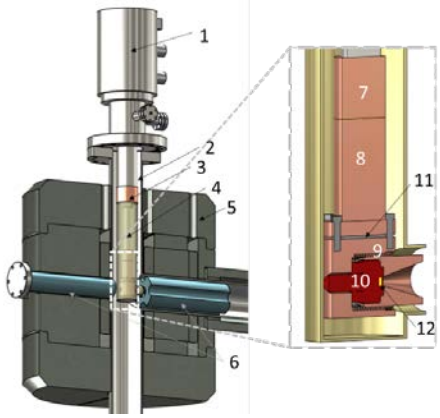

Fig. 1. Conceptual design of the ^{22}Na source chamber: 1) cryocooler head; 2) vacuum chamber (cross section); 3) cryocooler 1st stage cold place; 4) thermal radiation shield; 5) Pb gamma radiation shield (cross section); 6) in vacuum Elkonite radiation shield; 7) cryocooler 2nd stage cold place; 8 & 9) extensions of the 2nd stage cold place; 10) capsule for ^{22}Na source; 11) sapphire electrical insulation between 8 and 9; 12) radioactive material.

The conceptual design for the ^{22}Na source chamber for the ELI-NP positron laboratory is shown in Fig. 1. The shields sizes are calculated for safe operation with 50 mCi source. The main element of the cryogenic cooling system is the 4.2 K cryocooler, which is a standard closed-cycle, dual-stage heat pump, of Gifford-McMahon (GM) type. For an efficient slow e^+ beam formation, the ^{22}Na capsule part has to be set at a positive electric potential (~10^2 V), which with surrounding ground potential will form electric field accelerating the positrons. The electrical decoupling is made with a sapphire insulation. In order to control the sample temperature (6…10 K), an electric heater placed on the heat sink is used, which works together with a temperature controller adequate to the cryogenic temperature range. The entire cryocooler-thermal extension is surrounded by a thermal shield cooled by the 1st stage of the cryocooler that retains the thermal radiation from the enclosure to the assembly, which is at room temperature.

2.2. The conceptual design for the CMA chamber

Details on the CMA geometry, slow e^+ production (without neon moderation) and simulations on the extraction of the slow e^+ are published in [11, 17]. As it was already discussed in the Introduction, the rationale for considering an advanced CMA chamber design with neon moderation is based on the very low thermal load from the gamma rays interacting with the foils of the CMA [12]. The principal of operation is similar to what is described in section 2.1. However, in the present case the CMA is mounted at the cold finger extension and the fast e^+ will be created by the interaction of gamma rays with the CMA foils. The conceptual design is presented in Fig. 2.

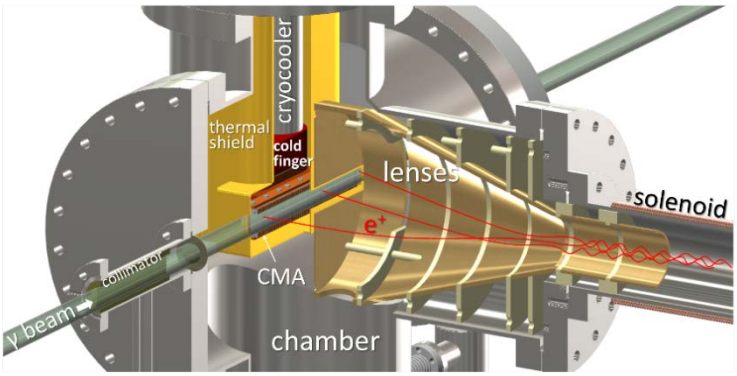

Fig. 2. Conceptual model of the CMA chamber. Please note that the chamber, thermal shield, collimator and lenses are shown as cross sections.

The solid neon layer formed on the surface of the foils will acts as a moderator. The moderated slow e^+ is focused by a system of lens, and the formed

a beam is magnetically guided by a system of solenoidal coils. Other differences lay in the shape, geometric dimensions of the cryogenic temperature parts, and in the cooling power and the type of the cryocooler. The additional condition imposed on the CMA chamber is the required reduced level of the vibrations produced by the cryocooler head body. The required low vibrations levels arise from the fact that the CMA chamber is in mechanical contact with the delicate recirculator of the gamma beam system [18]. One possible solution is to use a GM type cryocooler with a dedicated vibration damper or a Pulsing Tube type cryocooler, which generates vibrations 10 times weaker that the standard GM cryocoolers [19].

3. Numerical Simulations

The developed conceptual models underpin the numerical modeling based on a finite element method (FEM) [20] within the present stage. The thermal loads for the cryocooling systems and the thermal profile of the cold pieces and in particular the custom extensions of the cold finger are the object of the numerical study described in this section. Previous works confirm the appropriateness of the approach [21, 22].

3.1. Mathematical model

The numerical simulations consist in the heat transfer analysis of the stability of the system, and the evaluation of the heat loads that occur. The heat transfer occurs through conduction within the solid body parts and is described by the equation

$$\nabla \cdot (-k\nabla T) = 0, \tag{1}$$

and the radiation between surfaces and boundary to the ambient, governed by the equations

$$-\mathbf{n} \cdot (-k\nabla T) = h(T_{\text{inf}} - T) + \varepsilon(G - \sigma T^4), \tag{2}$$

$$(1-\varepsilon)G = J_0 - \varepsilon\sigma T^4, \tag{3}$$

where k [W m^{-1}K^{-1}] is the thermal conductivity, T [K] is the temperature, h [W m^{-2}K^{-1}] is the convection heat transfer coefficient, T_{inf} is the reference temperature, G [W m^{-2}] is the irradiation flux, ε is the surface emissivity, T_{amb} is the ambient temperature, J_0 [W m^{-2}] is the surface radiosity, and $\sigma = 5.67\times10^{-8}$ [W m^{-2}K^{-4}] is the Stefan – Boltzmann constant. The implicit boundary condition is thermal insulation.

3.2. ^{22}Na source chamber case

Figure 3.a presents the ^{22}Na source cryostat (the vacuum chamber) as a simplified CAD model, prepared from the conceptual design shown in Fig. 1,

together with the cryocooler, the thermal shield and the sample (from here now, under the term “sample” we will understand the cold place in combination of its extension). The tungsten foils of the CMA are considered as 72 individual foils (simulation accounts for only a part of these foils, to simplify the model) with an emissivity of $\varepsilon = 0.04$. Heat transfer through radiation occurs between the cryostat and the thermal shield, and between the thermal shield and the sample. The cryostat is made of stainless steel, with $\varepsilon = 0.12$, and the thermal shield is copper, with $\varepsilon = 0.02$. The thermal properties of the materials are loaded from the material library of [20]. Thus, cooling the system is made by conduction, from the two cooling stages of the cryocooler to the thermal shield (50 K) and to the sample (4.2 K). The two cold heads of the cryocooler have fixed temperatures (50 K, respectively 4.2 K), while the temperature distribution in the system is obtained through numerical modeling taking in consideration adequate subdomain and boundary conditions.

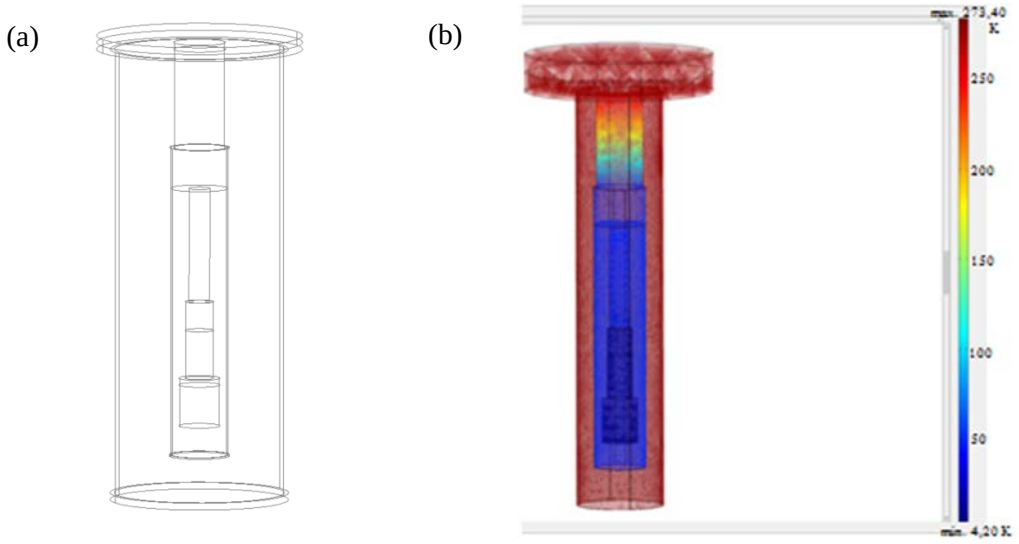

Fig. 3. (a) ^{22}Na source chamber – computational domain. (b) Surface temperature distribution.

Figure 3.b shows the temperature distribution in the cryogenic system for the ^{22}Na source chamber. It can be seen that the minimum temperature at the sample can be kept at 4.2 K. The thermal loads, which are obtained by the numerical simulations, on the two cooling stages of the cryocooler for the source are 2.27 W in the 1st stage of cooling, and 0.23 W in the 2nd stage of cooling.

3.3. CMA chamber case

Figure 4 shows a detail of Fig. 2, namely the CMA mounted on the cold finger extension together with a part of the thermal shield surrounding it. As can be seen, the shield has two smaller and one bigger opening. The smaller openings

are the gamma beam entrance and exit, and the big opening provides for the extraction of the moderated e^+. Actually, the big opening will be fully covered with a high transparency fine metal mesh (> 90% optical transparency, 30 LPI). As it is difficult to include the fine mesh in the model, two scenarios are studied. The first scenario considers the mesh as a good thermal shield (Fig. 5,a). In the second one the mesh is omitted (Fig. 5,b), and will be a source of additional thermal load to the 2nd stage of the cryocooler due to the direct exposure of the CMA foils to room temperature radiation from the other components.

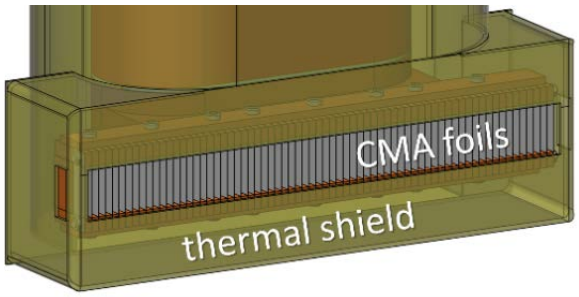

Fig. 4. CMA mounted on the cold finger extention with the thermal shield.

The computational domain presented in Fig. 5 is a simplified representation of the conceptual design shown in Fig. 2. Also, using the symmetry of the model, the full computational domain was reduced at half its size to simplify the numerical modeling problem. The material properties and boundary conditions are taken as explained in the section 3.2.

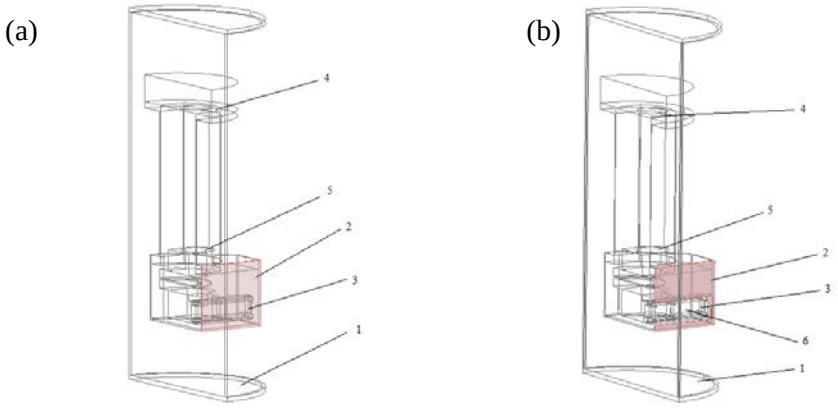

Fig. 5. Computational domain in the case of CMA chamber setup consists of a cryostat (1), a thermal shield (2) /the front face is shaded/, CMA (3) and a cryocooler with two cooling stages, 1st stage at 50 K (4) and the 2nd stage at 4.2 K (5). The setup (a) is with full thermal shield and (b) shows the thermal shield with opening (6).

The thermal loads on the cryocooler stages as obtained by the numerical simulations are presented in Table I.

Table I

CMA setup cryocoolers thermal loads as obtained by numerical simulations

Cooling stage	Thermal load (W)	
	no opening	with opening
1st (50 K)	2.16	3.5
2nd (4.2 K)	0.12	0.31

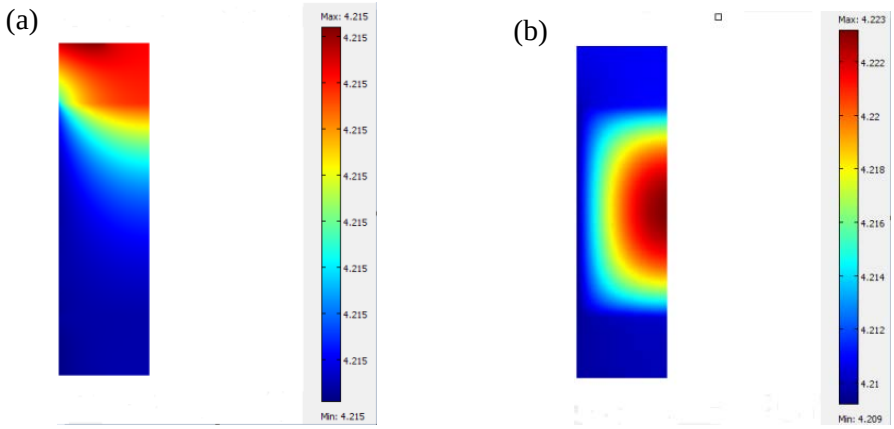

Fig. 6. Temperature distribution on the surface of the tungsten CMA foils in the case of thermal shield without (a) and with opening (b).

The temperature on the tungsten foil (Fig. 6) has a small variation exceeding 4.2 K as a result of the influence of the radiation (at room temperature) passing through the opening in the thermal shield. However, the excess is of the order of few hundreds of mK, and we may conclude that the opening in the thermal shield will not lead to any problem in condensation of the neon gas on the foils surfaces due to temperature issue.

4. Conclusions

This paper analyzes a cryogenic cooling system of a positron source, which will be the subject of specific experiments within the ELI-NP project in Măgurele. Two cases are presented: (1) a ^{22}Na positron source, and (2) a tungsten-based positron source. In both cases, it is necessary to have a thin layer of solid neon on either the ^{22}Na source or on the tungsten plates as moderator for positrons. Neon is deposited directly on the area of interest as a result of condensation and solidification at a temperature of 5-7 K directly on the positron emission area (as a result of radiant irradiation γ). Ensuring the required

temperature for the positron source will be accomplished using a G-M type cryocooler with two cooling stages: 1st stage at 50 K and the 2nd stage at 4.2 K.

The positron source will be cooled by thermal coupling of the positron source to the cryocooler cooling stage 2. Thermal control will be provided by a Lake Shore temperature controller, which acts on a heater placed between the cold head 2 of the cryocooler and the positron source.

The paper reports also the numerical modeling performed of the thermal loads of the two cooling stages of the cryocooler, which is a main concern. Thus, in the case of the ^{22}Na source, 0.23 W at 4.2 K and 2.27 W at 50 K respectively were obtained. For CMA source values of 0.31W at 4.2K, in case of rectangular window in the front of the tungsten plates, and 0.12 at 4.2 K respectively for the full thermal shield case.

The increase of the thermal load in the case of the necessary practiced window in the thermal shield is not very important, the total thermal load remaining below 1.5 W, which is the maximum thermal power of the cryocooler cooling stage 2 at 4.2 K. In this situation the condition required by the positron source temperature for proper condensation of the neon gas is satisfied.

Acknowledgements

The authors wish to acknowledge, the funding of this work by the Research and Innovation Ministry, under the contract E27/2016, in the frame of the ELI-RO Program.

R E F E R E N C E S

[1] *P.a.M. Dirac*, "On the Annihilation of Electrons and Protons", in Mathematical Proceedings of the Cambridge Philosophical Society, **vol. 26**, 2008, pp. 361-375

[2] *C.D. Anderson*, "The Positive Electron", in Phys. Rev., **vol. 43**, 1933, pp. 491-494

[3] *R.H. Howell, I.J. Rosenberg and M.J. Fluss*, "Production and Use of Low-Energy, Monoenergetic Positron Beams from Electron Linacs", in Applied Physics A, **vol. 43**, 1987, pp. 247-255

[4] *T. Hyodo, K. Wada, A. Yagishita, T. Kosuge, Y. Saito, T. Kurihara, T. Kikuchi, A. Shirakawa, T. Sanami, M. Ikeda, S. Ohsawa, K. Kakihara and T. Shidara*, "Kek-Imss Slow Positron Facility", in J. Phys.: Conf. Ser., **vol. 262**, 2011, pp. 012026

[5] *R. Suzuki, T. Ohdaira, T. Mikado, A. Uedono, H. Ohgaki, T. Yamazaki and S. Tanigawa*, "Moderation of Positrons Generated by an Electron Linac ", in Mater. Sci. Forum, **vol. 255-257**, 1997, pp. 114-118

[6] *A. Van Veen, F. Labohm, H. Schut, J. De Roode, T. Heijenga and P.E. Mijnarends*, "Testing of a Nuclear-Reactor-Based Positron Beam", in Appl. Surf. Sci., **vol. 116**, 1997, pp. 39-44

[7] *C. Hugenschmidt, H. Ceeh, T. Gigl, F. Lippert, C. Piochacz, P. Pikart, M. Reiner, J. Weber and S. Zimnik*, "The Upgrade of the Neutron Induced Positron Source Nepomuc", in J. Phys.: Conf. Ser., **vol. 443**, 2013, pp. 012079

[8] *I.H. Ayman, W.G. David, M. Jeremy, G.H. Alfred and M. Saurabh*, "Operation and Testing of the Pulstar Reactor Intense Slow Positron Beam and Pals Spectrometers", in J. Phys.: Conf. Ser., **vol. 262**, 2011, pp. 012024

[9] *J. Störmer, A. Goodyear, W. Anwand, G. Brauer, P.G. Coleman and W. Triftshäuser*, "Silicon

Carbide: A New Positron Moderator", in J. Phys.: Condens. Matter, **vol. 8**, 1996, pp. L89

[10] *A.P. Mills and E.M. Gullikson*, "Solid Neon Moderator for Producing Slow Positrons", in Appl. Phys. Lett., **vol. 49**, 1986, pp. 1121-1123

[11] *N. Djourelov, A. Oprisa and V. Leca*, "Source of Slow Polarized Positrons Using the Brilliant Gamma Beam at Eli-Np. Converter Design and Simulations", in Nucl. Instr. Meth. A, **vol. 806**, 2016, pp. 146-153

[12] *N. Djourelov, C. Hugenschmidt, S. Balascuta, V. Leca, A. Oprisa, C. Piochacz, C. Teodorescu and C.A. Ur*, "Positron Production by Gamma Beam at Eli–Np", in Rom. Rep. Phys., **vol. 68**, 2016, pp. S735-S797

[13] *Y.C. Wu, Y.Q. Chen, S.L. Wu, Z.Q. Chen, S.J. Wang and R.G. Greaves*, "High Moderation Efficiency Positron Beamline", in Phys. Status Solidi C, **vol. 4**, 2007, pp. 4032-4035

[14] *M. Weber, A. Schwab, D. Beckek and K.G. Lynn*, "Solid Neon Moderated Electrostatic or Magnetic Positron Beam", in Hyperfine Interact., **vol. 73**, 1992, pp. 147-157

[15] *R. Khatri, M. Charlton, P. Sferlazzo, K.G. Lynn, A.P. Mills Jr and L.O. Roellig*, "Improvement of Rare-Gas Solid Moderators by Using Conical Geometry", in Appl. Phys. Lett., **vol. 57**, 1990, pp. 2374-2376

[16] *P. Horodek, A.G. Kobets, I.N. Meshkov, A.A. Sidorin and O.S. Orlov*, "Slow Positron Beam at the Jinr, Dubna", in Nukleonika, **vol. 60**, 2015, pp. 725-728

[17] *N. Djourelov, A. Oprisa and V. Leca*, "Project for a Source of Polarized Slow Positrons at Eli-Np", in Defect and Diffusion Forum, **vol. 373**, 2017, pp. 57-60

[18] *O. Adriani, S. Albergo, D. Alesini, M. Anania, D. Angal-Kalinin, P. Antici, A. Bacci, R. Bedogni, M. Bellaveglia, C. Biscari, N. Bliss, R. Boni, M. Boscolo, F. Broggi, P. Cardarelli, K. Cassou, M. Castellano, L. Catani, I. Chaikovska, E. Chiadroni, R. Chiche, A. Cianchi, J. Clarke, A. Clozza, M. Coppola, A. Courjaud, C. Curatolo, O. Dadoun, N. Delerue, C.D. Martinis, G.D. Domenico, E.D. Pasquale, G.D. Pirro, A. Drago, F. Druon, K. Dupraz, F. Egal, A. Esposito, F. Falcoz, B. Fell, M. Ferrario, L. Ficcadenti, P. Fichot, A. Gallo, M. Gambaccini, G. Gatti, P. Georges, A. Ghigo, A. Goulden, G. Graziani, D. Guibout, O. Guilbaud, M. Hanna, J. Herbert, T. Hovsepian, E. Iarocci, P. Iorio, S. Jamison, S. Kazamias, F. Labaye, L. Lancia, F. Marcellini, A. Martens, C. Maroli, B. Martlew, M. Marziani, G. Mazzitelli, P. Mcintosh, M. Migliorati, A. Mostacci, A. Mueller, V. Nardone, E. Pace, D.T. Palmer, L. Palumbo, A. Pelorosso, F.X. Perin, G. Passaleva, L. Pellegrino, V. Petrillo, M. Pittman, G. Riboulet, R. Ricci, C. Ronsivalle, D. Ros, A. Rossi, L. Serafini, M. Serio, F. Sgamma, R. Smith, S. Smith, V. Soskov, B. Spataro, M. Statera, A. Stecchi, A. Stella, A. Stocchi, S. Tocci, P. Tomassini, S. Tomassini, A. Tricomi, C. Vaccarezza, A. Variola, M. Veltri, S. Vescovi, F. Villa, F. Wang, E. Yildiz and F. Zomer*, "Technical Design Report Eurogammas Proposal for the Eli-Np Gamma Beam System", in CORD Conference Proceedings, **vol.**, 2014, pp.

[19] Shi Cryogenics, http://www.shicryogenics.com/

[20] Comsol Multiphysics®, Comsol 4.3, Comsol Ab, Stockholm, Sweden, 2012

[21] *I. Dobrin, A. Chernikov, S. Kulikov, et all.*," A 4T HTS Magnetic Field Generator, Conduction Cooled, for Neutron Physics Spectrometry", IEEE Transactions on Applied Superconductivity : 2016, Volume: 26, Issue:3, Article 4500404, DOI: 10.1109/TASC.2016.2520086.

[22] *I. Dobrin, A.M.Morega, et all.* "A Conduction Cooled High Temperature Superconductor Quadrupolar Superferric Magnet. Design and Construction",11th European Conference on Applied Superconductivity (EUCAS), Genoa, ITALY, 2013, Journal of Physics Conference Series Volume:507, Article Number:032014, 2014.